Dust mode in collisionally dominated complex plasmas with particle drift.

S. Ratynskaia, M. Kretschmer, S. Khrapak, R. Quinn, M. Thoma, G. Morfill,
A. Zobnin, A. Usachev, O. Petrov, and V. Fortov

Abstract— **Experiments with micropareticles flow were conducted in a DC discharge. A sharp threshold in the neutral gas pressure for the onset of an unstable dust wave mode was observed. Highly space and time resolved measurements of the microparticle flow combined with probe measurements of the plasma parameters have allowed detailed comparison with a theoretical model. The model demonstrates good qualitative and quantitative agreement with the experimental data providing accurate estimates of the particle charge.**

Index Terms— **dust waves, particle charge**

mds
June, 2003

I. Introduction

It is well known that the presence of the microparticles in plasmas not only modifies some properties of the collective plasma wave modes, but also gives rise to low-frequency modes which essentially involve the dust dynamics. These low-frequency dust modes have been observed in many laboratory experiments [1]–[6]. In the majority of the experiments, waves were studied in stationary dust clouds confined by the balance of external forces (e.g. electric field, gravity, ion drag etc). In this paper we perform experiments with very small particles in a horizontal DC discharge tube where the force due to the weak (ambipolar) radial electric field in the bulk plasma compensates gravity. Another distinct feature of the experiment is a particle flow velocity much larger than the particle thermal velocity. Highly space and time resolved measurements provide information about the particle flow (flow velocity, particle number density) and wave properties (wavelength and phase velocity). Combining this with probe measurements of the plasma parameters, we are in a position for detailed comparisons with a theory. The used theoretical model is not only capable of reproducing the main qualitative features of the observations, but also gives quantitative results in good agreement with the experiment and hence yields accurate estimates of the particle charge.

II. Experimental set-up

The experiments are performed in a DC discharge in a 35 cm long U - shaped glass tube (PK-4 experiment). The set-up is sketched in Fig. 1 and details on the experimental facility PK-4 can be found in Ref. [7]. Injected particles (with number density varied) were caught by the plasma and, being charged negatively, were drifting against the discharge electric field in the horizontal part of the tube (see Fig. 1). We used standard Melamine-Formaldehyde particles with mass density $\rho_d = 1.51$ g/cm^3 and radius of $a = 0.6$ μm. The discharge was operated in Neon in the pressure range from 100 to 30 Pa with a discharge current of 1 mA. For $p = 50$ Pa, the probe measurements gave the following plasma parameters (details will be published elsewhere, see also Ref. [8]): Ion and electron density $n_i \simeq n_e \simeq 5 \times 10^8$ cm^{-3}, electron temperature $T_e \simeq 4.5$ eV and electric field $E \approx 2$ V/cm. The ion temperature T_i was not measured but for the pressures used it is reasonable to assume that it is close to the temperature of the neutral component, $T_i \simeq T_n \simeq 0.03$ eV.

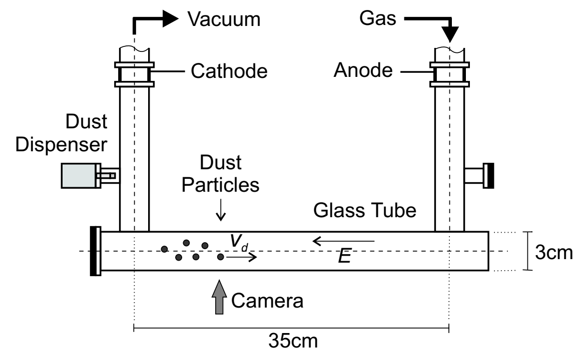

Fig. 1. Sketch of the experimental set-up (PK4 prototype chamber).

The particle motion was recorded by CCD camera with field of view of 640×480 pixels (corresponding approximately to 6.4 by 4.8 mm), and time resolution of 8.3 ms. The width of the laser sheet was 100 μm. The measurements were taken with the camera located at the position 12 cm from the cathod end of the main tube (see Fig. 1). It was checked that the dynamics is essentially the same along the rest of the glass tube.

III. Main features of the experiment

Here we discuss the experimental results obtained from an analysis of the digitized video. First, the dust number density was estimated to be $n_d \simeq 1.2 \times 10^5$ cm^{-3}, by counting the number of particles (approximately 600) in single snapshots of the video. An upper limit of uncertainty in n_d is 50 %. Second, wavelength λ (wave number k) and phase velocity $v_{ph} = \omega/k$ were obtained from the video sequences by analyzing the motion of the wave fronts and spacing between them. Lastly, particle velocities V_d were obtained by tracking individual particles through the video sequences. The results were obtained for a set of pressures in the range $30 - 100$ Pa.

Manuscript received xxxxx XX, 2003; revised xxxxx XX, 2003.

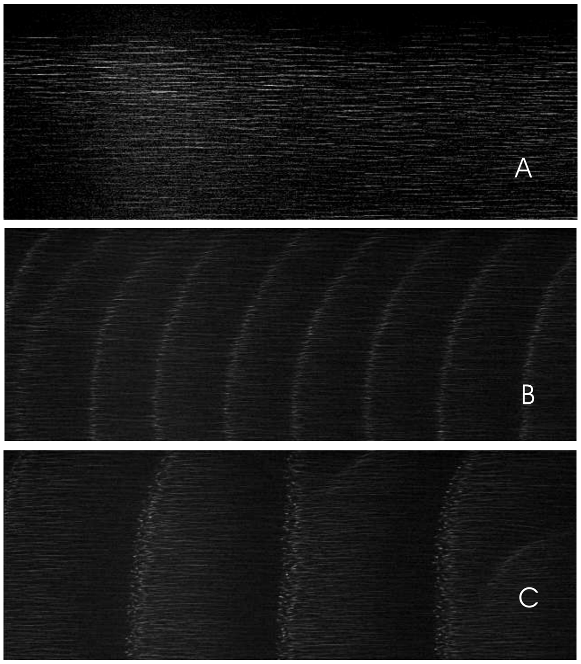

Fig. 2. Particle flow just above the threshold [$p \simeq 60$ Pa] (a), at the threshold [$p \simeq 55$ Pa] (b) and below the threshold [$p \simeq 50$ Pa] (c). Field of view is 4.8 by 6.4 mm. The center of the tube is located at the lower edge of the pictures. Direction of the electric field and the particle velocity in (a)-(c) is the same as in Fig. 1. Wave propagates to the left in (b) and to the right in (c). For (b): wave length $\lambda \simeq 0.08$ cm, phase velocity $v_{ph} = \omega/k \simeq 0.24$ cm/s, wave frequency $\omega \simeq 80$ s^{-1} and particle velocity $V_d \simeq 4$ cm/s. For (c): $\lambda \simeq 0.18$ cm, $v_{ph} \simeq 0.50$ cm/s, $\omega \simeq 17$ s^{-1} and $V_d \simeq 5.5$ cm/s.

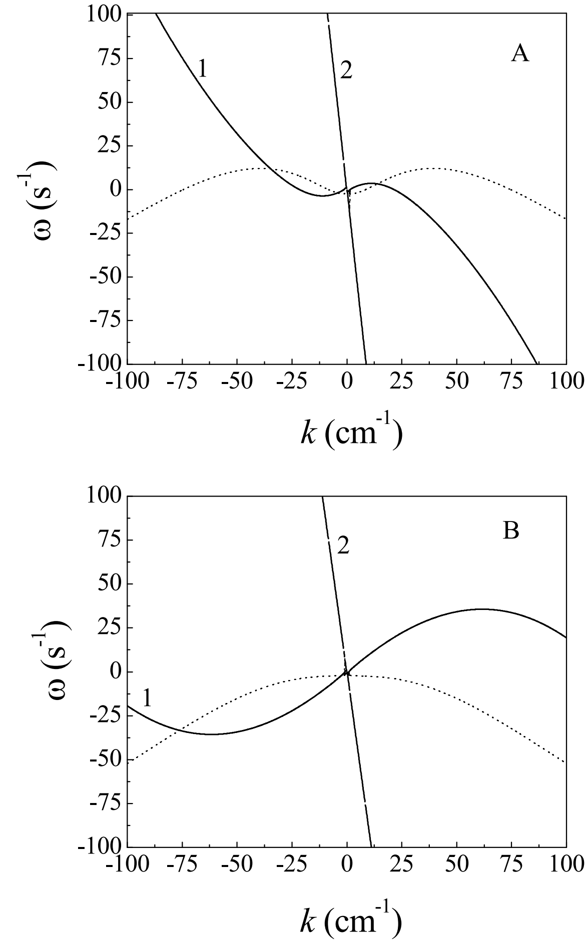

Fig. 3. Numerical solution of the dispersion relation [Eq. (1)] for $p = 50$ Pa (a) and $p = 60$ Pa (b). Real and imaginary parts of ω are given by solid and dashed lines, respectively. Curves 1 correspond to "low-frequency" mode and curves 2 to strongly damped "high-frequency" mode.

The following main features of the overall experiment were observed:

1. A sharp threshold for wave generation, with decreasing pressure, at $p \simeq 55$ Pa was detected. Fig. 2 (a) shows an undisturbed particle flow for a pressure $p \simeq 60$ Pa and Figs. 2 (b) and (c) present the situation when an instability takes place.

2. Right at the threshold [$p \simeq 55$ Pa, Fig. 2(b)] the particles and the wave fronts are moving in opposite directions. Below the threshold, the wave fronts are moving in the same direction as the particles [Fig. 2(c)].

3. Below the threshold, the waves propagate faster and the wave length is longer compared to that at the threshold (see caption to Fig. 2).

4. Similar to previous works [4], we observe that the threshold shifts towards higher pressures when the number of the particles is increased.

IV. Comparison with theory

In deriving a theoretical dispersion relation, we take into account the following effects: Ion-neutral and dust-neutral collisions, and ion and dust particle drift in the discharge electric field. We assume Boltzmann distribution for electrons in the wave potential and neglect ion inertia as the limit of very low frequency waves (on the electron and ion frequency scale) is considered. We also assume cold dust fluid (omitting the pressure term in the momentum equation for the particles). The effects of nonideality of the particle component are neglected, which seems to be reasonable because we are dealing with collisionally dominated plasma (see e.g., Ref. [9]). The resulting linear dispersion relation within the hydrodynamic approach is similar to that derived in Ref. [6] (the only modification takes accounts of the particle drift with velocity V_d), and can be written in the form

$$1 + \frac{1}{k^2\lambda_{\rm De}^2} + \frac{\omega_{pi}^2}{k^2 v_{T_i}^2 + k u_0 (i\nu_{in} - k u_0)} - \frac{\omega_{pd}^2}{(\omega + kV_d)(\omega + kV_d + i\nu_{dn})} = 0 \qquad (1)$$

where $\lambda_{\rm De} = \sqrt{T_e/4\pi e^2 n_e}$ is the electron Debye radius, $\omega_{pi} = \sqrt{4\pi e^2 n_i/m_i}$ is the ion-plasma frequency, u_0 and $v_{T_i} = \sqrt{T_i/m_i}$ are the ion drift and thermal velocity, and m_i is the ion mass. The dust plasma frequency is $\omega_{pd} = \sqrt{4\pi Z^2 e^2 n_d/m_d}$, where Z and m_d are the particle charge number and mass, respectively. The momentum transfer frequency for dust-neutral and ion neutral collisions are $\nu_{in} \simeq n_n \sigma_{in} v_{T_i}$ and $\nu_{dn} = (8\sqrt{2\pi}/3)a^2 n_n v_{T_n}(m_n/m_d)$, where n_n, v_{T_n}, m_n are the density, thermal velocity, and mass of neutrals, and σ_{in} is the momentum-transfer cross section for ion-neutral collisions.

With the plasma parameters given in Sec. II we estimate

$\lambda_{\rm De} \simeq 700$ μm, $\lambda_{\rm D\it i} \simeq 60$ μm, $v_{T_i} \simeq 3.8 \times 10^4$ cm/s, and $\omega_{pi} \simeq 6.5 \times 10^6$ s^{-1}. The ion drift velocity can be then calculated using the measured value of the electric field, $u_0 = eE/m_i\nu_{in}$. For the estimations, $\sigma_{in} \simeq 10^{-14}$ cm^2 is taken for the effective ion-neutral momentum transfer cross section in Neon. The particle drift velocity is measured in the experiment. The values of the characteristic momentum-transfer frequencies and drift velocities for the ion and particle components are given in Table I for two values of the neutral gas pressure, $p = 60$ Pa (above the threshold) and $p = 50$ Pa (below the threshold). Using these values the dispersion relation (1) can be solved numerically for any given ω_{pd}. Matching the experimental results with the solution we can estimate the dust-plasma frequency and, hence, the particle charge.

The numerical solution of the dispersion relation reproducing the main qualitative and quantitative features of the experiment is presented in Figs. 3 (a) and (b) for the pressures $p = 50$ and $p = 60$ Pa, respectively. It corresponds to $\omega_{pd} \simeq 900$ s^{-1}. We can observe that two solutions exist. One is a "high frequency" acoustic-like mode (curves 2). It is highly damped (the damping rate is very large and is not shown in Fig. 3 for clarity) for both pressures and is of no interest for the present analysis. The other is non-acoustic "low frequency" mode and below we analyze its behavior. For lower pressure ($p = 50$ Pa) this mode can propagate in the direction opposite to the electric field ($\omega > 0$, $k < 0$). It is unstable for a range of wave numbers, with the maximum increment at $k \simeq 40$ cm^{-1} [see Fig. 3 (a)]. The most unstable mode is characterized by the phase velocity $v_{ph} \simeq 0.45$ cm/s. Both values are very close to the experimental observations (see caption to Fig. 2). The wave behavior changes as the pressure is increased. It follows from Fig. 3 (b) that at the pressure $p = 60$ Pa, the wave can propagate in the direction of the electric field ($\omega > 0$, $k > 0$), i.e. opposite to the previous case, however it is damped for all k. This implies that the transition to the wave instability should occur somewhere between $p = 50$ Pa and $p = 60$ Pa, in good agreement with the observations.

We can estimate particle charge using the fact that good agreement between theory and experiment was obtained at $\omega_{pd} \simeq 900$ s^{-1}. With the measured value of the particle number density, $n_d \simeq 1.2 \times 10^5$, we find the particle charge number to be $Z \simeq 2.0 \times 10^3$. This is smaller than the value calculated from the orbital motion limited (OML) theory ($Z_{\rm OML} \simeq 4 \times 10^3$) by approximately a factor of two. This result seems to be in reasonable agreement with the recent calculations [10], [11] which predict a decrease in the particle charge due to ion-neutral (charge exchange) collisions.

V. Conclusion

Experiments with dust grain flows in a DC discharge are presented. A threshold in the neutral gas pressure for the onset of the dust wave instability was observed. Using accurate measurements of flow and plasma characteristics we are able to determine the particle charge from comparison between experiments and theoretical dispersion relation. The charge obtained is less than OML theory predicts which could be expected for the neutral pressure used in experiments. Preliminary investigations show that the theoretical model is also capable of describing more delicate features of the experiments like the changing direction of the wave propagation and shifting the threshold towards higher pressures with the dust number density increased. This work is in the progress and details will be published elsewhere.

TABLE I

Characteristic momentum-transfer frequencies and drift velocities for ion and dust components

p, Pa	u_0, cm/s	V_d, cm/s	ν_{dn},s^{-1}	ν_{in}, s^{-1}
50	1.9×10^4	5.5	298	5.0×10^6
60	1.6×10^4	4	358	6.0×10^6

Acknowledgment

The authors would like to thank Karl Tarantik and Yurii Gerasimov for skillful technical assistance.

References

[1] A. Barkan, R. L. Merlino, and N. D'Angelo, Phys. Plasmas **2**, 3563 (1995).
[2] C. Thompson, A. Barkan, N. D'Angelo and R. L. Merlino, Phys. Plasmas **4**, 2331 (1997).
[3] J. B. Pieper and J. Goree, Phys. Rev. Lett. **77**, 3137 (1996).
[4] V. I. Molotkov, A. P. Nefedov, V. M. Torchinskii, V. E. Fortov, and A. G. Khrapak, Zh. Eksp. Teor. Fiz. **116**, 902 (1999) (in Russian) [JETP **89**, 477 (1999)]
[5] V. E. Fortov *et al.*, Phys. Plasmas. **7**, 1374 (2000).
[6] S. Khrapak, D. Samsonov, G. Morfill *et al.*, Phys. Plasmas **10**, 1 (2003).
[7] R. A. Quinn *et al.*, Rev. Sci. Instr. (to be published); M. Kretschmer, PK4 Team: 'PK4 Homepage', http://www.mpe.mpg.de/pk4
[8] 2nd Milestown report for MPE, IHED, Moscow, May 2003.
[9] M. Rosenberg, and G. Kalman, Phys. Rev. E **56**, 7166 (1997)
[10] A. V. Zobnin, A. P. Nefedov, V. A. Sinel'shchikov, and V. E. Fortov, JETP **91**, 483 (2000)
[11] M. Lampe, R. Goswami, Z. Sternovsky, S. Robertson, V. Gavrishchaka, G. Ganguli, and G. Joyce, Phys. Plasmas **10**, 1500 (2003)]